ISME

www.nature.com/ismej

ARTICLE

Microbial gene expression in Guaymas Basin subsurface sediments responds to hydrothermal stress and energy limitation

Paraskevi Mara[1], Ying-Li Zhou[2], Andreas Teske[3], Yuki Morono[4], David Beaudoin[5] and Virginia Edgcomb[1]✉

Analyses of gene expression of subsurface bacteria and archaea provide insights into their physiological adaptations to in situ subsurface conditions. We examined patterns of expressed genes in hydrothermally heated subseafloor sediments with distinct geochemical and thermal regimes in Guaymas Basin, Gulf of California, Mexico. RNA recovery and cell counts declined with sediment depth, however, we obtained metatranscriptomes from eight sites at depths spanning between 0.8 and 101.9 m below seafloor. We describe the metabolic potential of sediment microorganisms, and discuss expressed genes involved in tRNA, mRNA, and rRNA modifications that enable physiological flexibility of bacteria and archaea in the hydrothermal subsurface. Microbial taxa in hydrothermally influenced settings like Guaymas Basin may particularly depend on these catalytic RNA functions since they modulate the activity of cells under elevated temperatures and steep geochemical gradients. Expressed genes for DNA repair, protein maintenance and circadian rhythm were also identified. The concerted interaction of many of these genes may be crucial for microorganisms to survive and to thrive in the Guaymas Basin subsurface biosphere.

The ISME Journal; https://doi.org/10.1038/s41396-023-01492-z

INTRODUCTION

Our overall knowledge of the diversity and in situ putative metabolisms of subsurface microorganisms in deep sea hydrothermal ecosystems derives to a large extent from culturing efforts and DNA-based surveys of hydrothermal sediments (reviewed in [1]). RNA-based investigations can inform on in situ activities of microorganisms. For hydrothermal settings, these are limited to metatranscriptome and cDNA marker gene studies of hydrothermal plume waters, vent chimneys, surficial microbial mats, and their underlying sediments sampled by submersible push cores (e.g., [2–6]), as well as RNA-based stable isotope probing experiments of hydrothermal fluids [7, 8]. These studies revealed expression of key genes involved in methane, sulfur, nitrogen and hydrogen cycling, and expression of heat shock proteins and proteases (e.g., [7]). Here we examine the total RNA pool from deep subsurface sediments (≥0.8 and up to 101.9 meters below sea floor; mbsf) that were drilled during International Ocean Discovery Program (IODP) Expedition 385 in Guaymas Basin, Gulf of California, Mexico, and we provide the first insights into gene expression in the deep biosphere of this hydrothermally active seafloor spreading center.

In the Guaymas Basin, basaltic intrusions and strong heat flow permeate its thick (>500 m thick) organic-rich sediments that derive from the productive overlying waters and from terrigenous inputs. These intrusions and the heat flow produce a spectrum of cold to hot seep sites, as well as hydrothermal hot spots with distinct thermal profiles and microbial communities in their surficial sediments (e.g., [9]). Pyrolysis of buried organic carbon at depth produces a complex milieu of liquid and dissolved petroleum hydrocarbons, including light hydrocarbons and methane, alkanes, and aromatic compounds, as well as carboxylic acids, and ammonia [10, 11]. These compounds are transported in hydrothermal fluids through Guaymas Basin sediments, supporting diverse microbial communities ([12, 13]) that include methanogens, chemoautotrophs [14], and deeply-branching archaeal lineages like Asgard archaea [15, 16].

During IODP 385, eight sites with distinct geological features and biogeochemical and thermal profiles, were drilled into the sedimented off-axis regions and axial trough of Guaymas Basin (sites U1545-U1552; Fig. 1, Table 1, Supplementary Table 1 and detailed in "Sample collection"). U1545 and U1546 are adjacent sites located ~52 km northwest of the northern Guaymas Basin axial trough. U1546 has a massive, thermally equilibrated sill between 350 and 430 mbsf that disrupts the sedimentary strata, and changes the physical properties and geochemical gradients of the sediment [17]. Sites U1547 and U1548 are ~27 km northwest of the axial trough, where a shallow, recently emplaced hot sill creates steep thermal gradients and drives hydrothermal circulation. Off-axis sites U1549 and U1552 are methane cold seep sites that are driven by deeply buried old sill

[1]Geology and Geophysics Department, Woods Hole Oceanographic Institution, Woods Hole, MA, USA. [2]Southern Marine Science and Engineering Guangdong Laboratory (Guangzhou), Guangzhou, China. [3]Department of Earth, Marine and Environmental Sciences, University of North Carolina, Chapel Hill, NC, USA. [4]Kochi Institute for Core Sample Research, Institute for Extra-cutting-edge Science and Technology Avant-garde Research (X-star), Japan Agency for Marine-Earth Science and Technology (JAMSTEC), Monobe, Nankoku, Kochi, Japan. [5]Biology Department, Woods Hole Oceanographic Institution, Woods Hole, MA, USA. ✉email: vedgcomb@whoi.edu

Received: 8 May 2023 Revised: 1 August 2023 Accepted: 2 August 2023
Published online: 01 September 2023

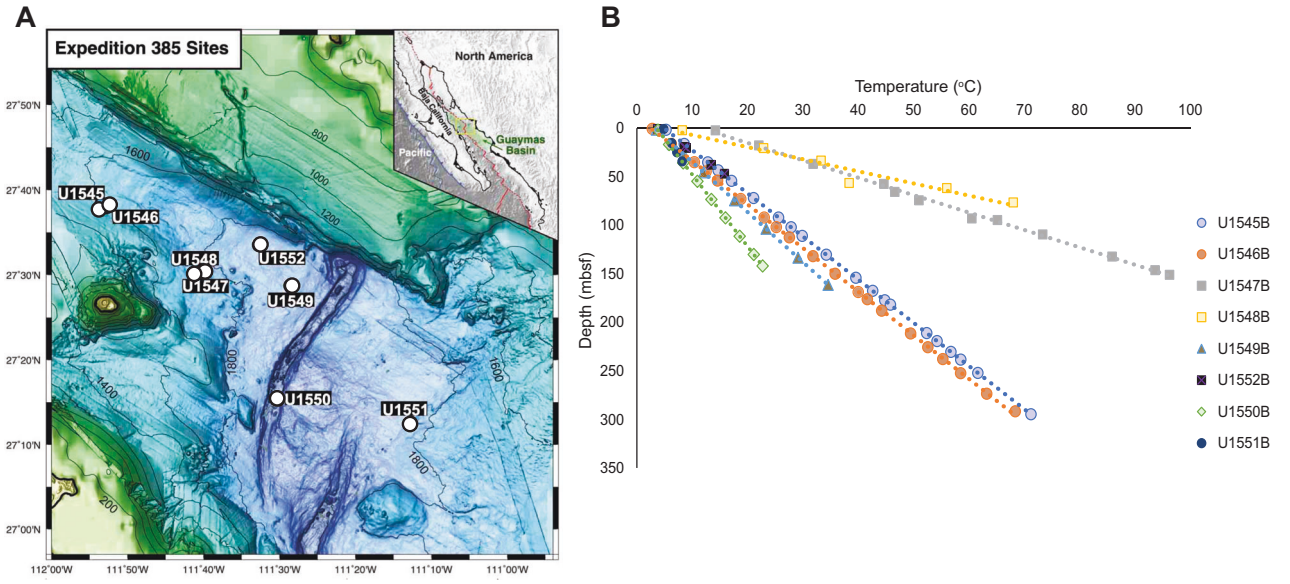

Fig. 1 Guaymas Basin overview. A Bathymetry of Guaymas Basin with IODP Expedition 385 drilling sites U1545 to U1552. Light green to deep blue contour lines indicate the increasing water depth in meters. The inner figure shows the overall sampling location in Guaymas Basin; red lines depict the transformation faults, and green lines show the oceanic spreading centers along the transformation faults in Guaymas Basin. Drilling sites included two adjacent sedimented sites in the northwestern flanking regions, with (U1546) and without (U1545) a deep sill intrusion at ~350-430 mbsf; two sites at the hydrothermally active Ringvent formation, where a shallow, recently emplaced hot sill creates steep temperature gradients and drives hydrothermal circulation (sites U1547 and U1548); one site 3.2 km offset from a cold seep on the northwestern flanking regions (U1549), and a cold seep site with a shallow hydrate area on the Sonora Margin (U1552). IODP 385 also drilled the northern axial valley (U1550) and the southwestern franking region known to receive terrestrial sediment input (U1551). **B** Temperature gradients in the Guaymas Basin subsurface (Source Data).

Table 1. Summary of location, water and drilling depths [52] of the IODP 385 sites.

Site	Hole	Latitude	Longitude	Water depth (mbsl)	Total penetration (mbsf)	Cored interval (mbsf)	Core recovered (mbsf)	SMTZ (mbsf)	Start (2019)	End (2019)
U1545	B	27°38.2301′N	111°53.3295′W	1594.24	387.3	387.3	340.1	50–80	1-Oct	4-Oct
U1546	B	27°37.8840′N	111°52.7809′W	1585.58	333.8	333.8	351.2	80–100	7-Oct	9-Oct
U1547	B	27°30.4128′N	111°40.7341′W	1732.22	209.8	209.8	161.3	99	16-Oct	20-Oct
U1548	B	27°30.2540′N	111°40.8601′W	1738.94	95.1	95.1	87.7	76	21-Oct	22-Oct
U1549	B	27°28.3383′N	111°28.7927′W	1841.17	166.9	166.9	164.4	30	25-Oct	27-Oct
U1550	B	27°15.1704′N	111°30.4451′W	2001.21	174.2	174.2	160.8	10	28-Oct	30-Oct
U1551	B	27°12.3832′N	111°13.1841′W	1843.9	48.5	48.5	50	25	3-Nov	4-Nov
U1552	B	27°33.2885′N	111°32.9640′W	1841.09	55	55	40	10	9-Nov	10-Nov

mbsl meters below sea level, *mbsf* meters below seafloor, *SMTZ* sulfate-methane transition zone.

intrusions. Off-axis site U1550 is located within the northern axial trough, and site U1551 in the southeastern Guaymas Basin is most strongly influenced by terrigenous input from the Sonoran Margin. We present messenger RNA (mRNA) evidence for metabolic activities of subsurface microorganisms using 19 metatranscriptomes prepared from shallow (0.8–2.1mbsf), intermediate (15.4-36.8 mbsf) and deeper depths (defined here as the deepest depths from which we extracted sufficient RNA for metatranscriptomics (74.2–101.9 mbsf), available only for sites U1545B, U1546B and U1547B). A detailed description and annotation of all transcripts discussed in this study can be found in Supplementary Tables 2 and 3. We aimed to identify major metabolic pathways used by active microbial groups, and to determine whether survival and activity was dominated by increasingly specialized microorganisms with increasing depth. Additionally, we investigated whether survival and activity depend on coordinated cellular responses that are widespread among bacteria and archaea – namely posttranscriptional tRNA and rRNA editing, mRNA degradation, DNA maintenance, and protein homeostasis.

RESULTS

Cell counts and taxonomy of transcripts

RNA recovery from our subsurface samples was challenging and declined with downcore depth, consistent with the overall ~1000-fold decrease in cell counts detected between the seafloor and ~100 mbsf (Fig. 2). At the hot Ringvent sites (U1547 and U1548) cell counts already decreased sharply from $>10^8$ to 10^6 cells cm^{-3} by the first ~60 mbsf (temperature up to ~56 °C). In contrast, a more gradual decline in cell abundance was detected at temperate sites where temperatures did not exceed 18°C between 0.8 and 60 mbsf (Fig. 2A). This trend supports the notion that in situ temperature, rather than depth, shapes cell density in these subsurface hydrothermal sediments (Fig. 2B). Putatively active taxa based on metatranscriptome data include methanogens/methanotrophs (Methanophagales, Methanococcales, Methanosarcinales), bacterial lineages previously identified in deep subsurface (Chloroflexota, Atribacteria, Planctomycetes, Aminicenantes), and archaeal taxa associated with anoxic/sulfidic and moderately thermophilic conditions (Lokiarchaea, Heimdallarchaeota, Thermoproteota, Bathyarchaeota) (Supplementary Table 2). DNA-based

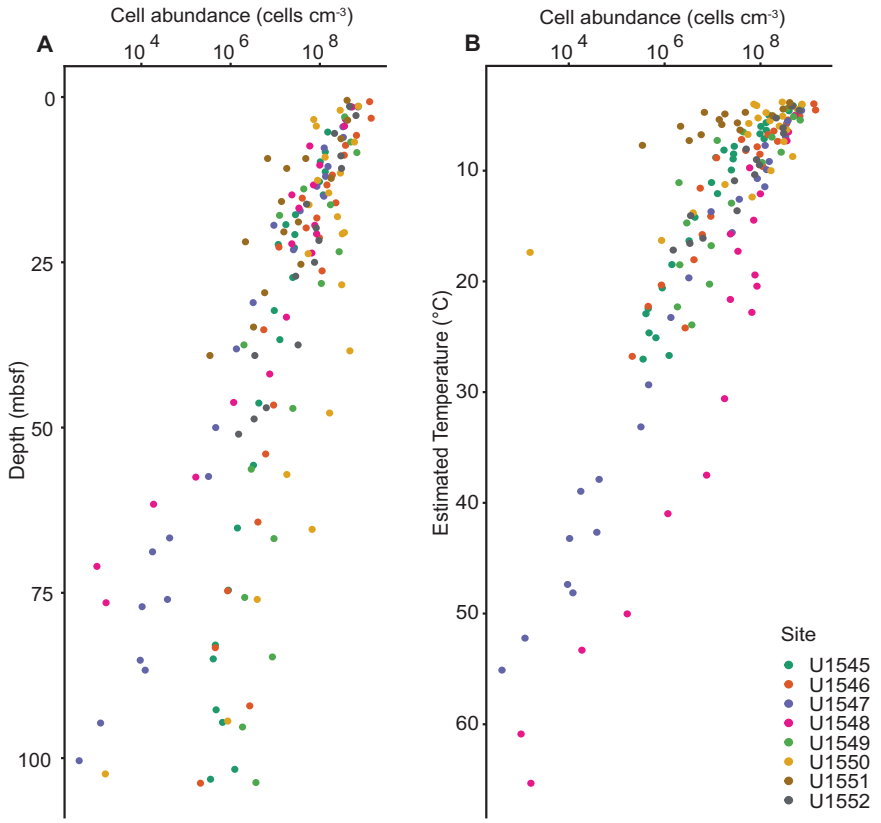

Fig. 2 Cell abundances for eight IODP385 drilling sites sampled for metatranscriptomic analysis. A Cell abundance data vs. depth. **B** Cell abundance data vs. temperature.

long-read sequencing (~800 base pairs) of the archaeal 16S rRNA gene confirms the presence of these archaeal taxa detected in the metatranscriptomes (Supplementary Fig. 1).

Metabolic processes that dominate in the Guaymas subsurface

In almost all samples, we find mRNA evidence for metabolic processes plausible for the deep biosphere, including methane, sulfur and nitrogen cycling, and chemoautotrophy (Fig. 3). We also observe expressed genes involved in biosynthetic pathways that produce cofactors that can support these metabolisms, and expressed genes associated with microbial defense, motility and chemotaxis that indicate an active subsurface community (Fig. 3). The identified processes and metabolisms are most highly expressed across our sites between 0.8 and 36.8 mbsf, before relative expression drops to near-zero at depths ≥92 mbsf at the northwestern off-axis sites, and at 74.2 mbsf in the hot Ringvent site U1547B. Although all samples were processed identically, the cDNA yield from sample U1546B at 16.2 mbsf was low, and sequencing yielded the lowest recovery of reads, precluding any detailed interpretation of data from that sample (Supplementary Table 4).

At the hot Ringvent sites U1547B and U1548B (>50 °C below 56 mbsf), key genes and co-factors that were associated with methanogenesis using different substrates (e.g., CO_2, acetate) were abundantly expressed at shallow and intermediate depths (Fig. 4). Methanogenesis-related genes were also expressed in shallow sediments from cold seep sites (e.g., U1549B and U1552B; 0.8–1.5 mbsf ~3.5 °C), sites enriched in terrigenous organic inputs (e.g., U1551B; 0.8 mbsf, 3.7 °C), and from shallow sediments of U1546B (Fig. 4). The lowest relative expression levels of genes for putative methanogenesis were detected in deeper samples, at 74.2 mbsf (~51 °C) in the hot Ringvent site U1547B, and at 92.1 mbsf (~25.6 °C) in the cooler site U1545B.

A wide range of expressed CO_2 fixation pathways including the Wood-Ljungdahl (WL) and 3-hydroxypropionate/4-hydroxybutyrate pathways, the reductive Krebs (rTCA) and dicarboxylate/4-hydroxybutyrate cycles (DC/4HB), and the 3-hydroxypropionate bi-cycle, was detected between 0.8 and 36.8 mbsf at almost all examined sites (Fig. 4). Site U1545B revealed relatively moderate gene expression for rTCA between 1.7 and 25.8 mbsf, and for WL at 25.8 mbsf (Fig. 4). At 92.1 mbsf (25.6 °C) low expression of rTCA is observed, and expression of DC/4HB (not observed at 1.7 and 25.8 mbsf) appears. At hot Ringvent site U1547B, chemoautotrophy genes are almost undetectable at 74.2 mbsf (51°C). Key genes involved in folate metabolism, one-carbon pool from folate metabolism, and the glycine cleavage system (that provides CO_2, NH_4 and -CH_2-groups; [18]) were co-expressed with genes associated with methane cycling and chemoautotrophy at depths between 0.8-36.8 mbsf at all sites (except U1545B; Figs. 3, 4). Folate-mediated C1 metabolism produces methyl/methylene groups that support microbial growth on C1 compounds (any reduction state from CO_2 to CH_4; [19]).

Key genes involved in nitrogen cycling showed generally low expression levels (Fig. 4). Co-expression of genes involved in putatively complete denitrification (*narG/H/I*, *napA/B, norB, nosZ*) was detected at the cold seep site U1549B at 1.5 mbsf. Hydroxylamine reductase (*hcp*) and hydroxylamine dehydrogenase (*hao*) genes involved in ammonia production, were moderately expressed at shallow and intermediate depths of sites U1549B and U1547B. We did not detect expressed genes for nitrification (e.g., ammonia oxygenases, *amo*), consistent with pervasive anoxia of Guaymas subsurface sediments. Relatively abundant expression levels of urea and ornithine cycling were detected in samples from almost all examined sites between 0.8 and 36.8 msbf.

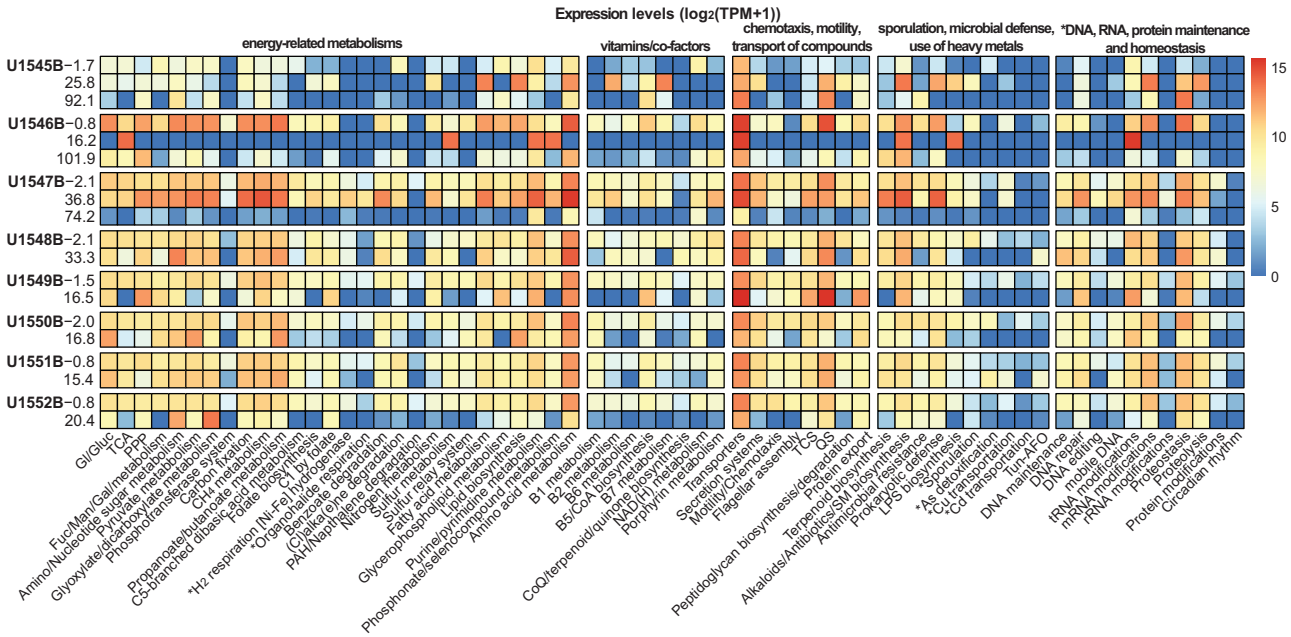

Fig. 3 Heatmap showing expression levels (log_2(TPM + 1)) of selected metabolic and cellular processes in Guaymas Basin subsurface sediment samples. Metabolic and cellular processes identified at the examined sites and depths using the KEGG database, and the BLASTx results generated with DIAMOND against NCBI-NR database (indicated with an asterisk). Processes involve pathways associated with energy-related metabolisms, genetic maintenance, survival strategies, and vitamin/co-factor biosynthesis (Supplementary Tables 2, 3, Source Data and "Methods"). Sites and depths are along the Y axis of the heatmap, and depths are given in meters below sea floor (mbsf). Expression levels are normalized as log_2 transformation of TPM + 1 (a value of 1 was added to TPM values to avoid zeros). TPM Transcripts Per Million, Gly/Gluc glycolysis/gluconeogenesis, TCA Krebs cycle, Fuc/Man/Gal Fructose/Mannose/Galactose, TCS two-component system, QS quorum sensing, As arsenic, Cu Copper, Cd cadmium, CoA Coenzyme A, CoQ complex Q, SM secondary metabolites, Tun-AFO Tungsten-containing aldehyde ferredoxin oxidoreductases.

Expressed genes for sulfate assimilation, and dissimilatory sulfate reduction to H_2S were detected at shallow depths at all sites, and at 15.4 and 36.8 mbsf at sites U1551B and U1547B, respectively. Sulfate assimilation was also detected below 90 mbsf at site U1546B, albeit at a relatively lower expression level (Fig. 4). The overall expression of genes associated with dissimilatory sulfate reduction was higher in shallow subsurface samples, where sulfate is available at near-seawater concentrations (Supplementary Table 1).

Links between RNA editing and subsurface metabolisms

RNA editing is an essential process detected in prokaryotes and eukaryotes that involves posttranscriptional modifications of tRNA, mRNA and rRNA molecules. In prokaryotes has been described using cultured bacterial and archaeal strains (see "Discussion").

These posttranscriptional modifications regulate RNA plasticity in cells and utilize methyl/methylene-groups that come from folate-mediated C1 metabolism (tetrahydrofolate) [20]. Our metatranscriptomes suggest active folate-mediated C1 metabolism in the Guaymas subsurface (Figs. 3, 4), which prompted us to manually search our BLASTx results for expressed RNA editing genes that encode proteins and tailoring enzymes that have been reported in the literature (Figs. 3, 6, Supplementary Table 2, and "Methods"). RNA editing genes modulate mRNA translation (via rRNA and tRNA editing) and mRNA degradation, which can both enhance survival in the Guaymas Basin subsurface biosphere (see "Discussion"). Expressed genes involved in mRNA degradation were primarily expressed by archaeal linages affiliated with Bathyarchaeota and the Asgard superphylum (Supplementary Table 2 for detailed annotations). Evidence for active tRNA modifications was also present at all examined depths in metatranscriptomes. These modifications were affiliated with various archaeal and bacterial linages previously reported in the deep biosphere (Fig. 3, Supplementary Table 2). Transcripts encoding a ribosomal silencing factor (rRNA modifications; Figs. 3, 6) were retrieved from shallow and intermediate depths at the hot Ringvent site U1547B and were annotated primarily to Atribacteria (Supplementary Table 2).

In archaea, the highly organized cellular process of mRNA degradation is mediated by exosomes, which are conserved protein machineries that share structural and functional similarities with the exosomes found in eukaryotes [21] (Fig. 5). Manual curation of the metatranscriptome data identified genes encoding for the exosomal proteins Rpr41, Rpr42 and Csl4. These genes were primarily expressed in shallow sediments (0.8–2.1 mbsf) (Fig. 6), and were annotated to Lokiarchaeota, Bathyarchaeota, and Heimdallarchaeota. Nonetheless, Rpr41, Rpr42, and Csl4 transcripts were retrieved also from deeper sediments at 33.3 and 36.8 mbsf (~32–33 °C) at hot Ringvent sites U1547B and U1548B, and at the cool site U1551B (6.3 °C) at 15.4 mbsf. Exosome-catalyzed mRNA degradation is also supported by the expression of bathyarchaeotal ski2-type helicase that clamps mRNA molecules to the exosomes, and by the expression of the lokiarchaeotal mRNA-cleaving ribonuclease aCPSF1, which is a transcription terminator that cleaves the 3′-end of the mRNA [22, 23]. The ski2-type helicase and aCPSF1 ribonuclease genes are co-expressed at shallow and intermediate depths at Ringvent sites U1547B (2.1–36.8 mbsf; 14.2–31.8 °C), and in the shallow, cool sediments of sites U1549B and U1550B (1.5–2 mbsf; ~3.5 °C) (Fig. 6). Other ribonucleases (e.g., Y, R, Z, D, P, PH, II, III, HIII, Y, E/G, MPR, VapC), and retrohoming endonucleases (degrade RNA and reintegrate introns into DNA; [24] were expressed abundantly at all Guaymas subsurface depths and sites, except from 74.2 mbsf at U1547B (Fig. 6; Supplementary Table 2).

Archaeal exosomes have functional (but not structural) similarities to the bacterial polynucleotide phosphorylase (PNPase) that degrades mRNA in bacteria [25, 26]. Expression of PNPase was observed in 13/19 metatranscriptomes (Fig. 6) indicating active

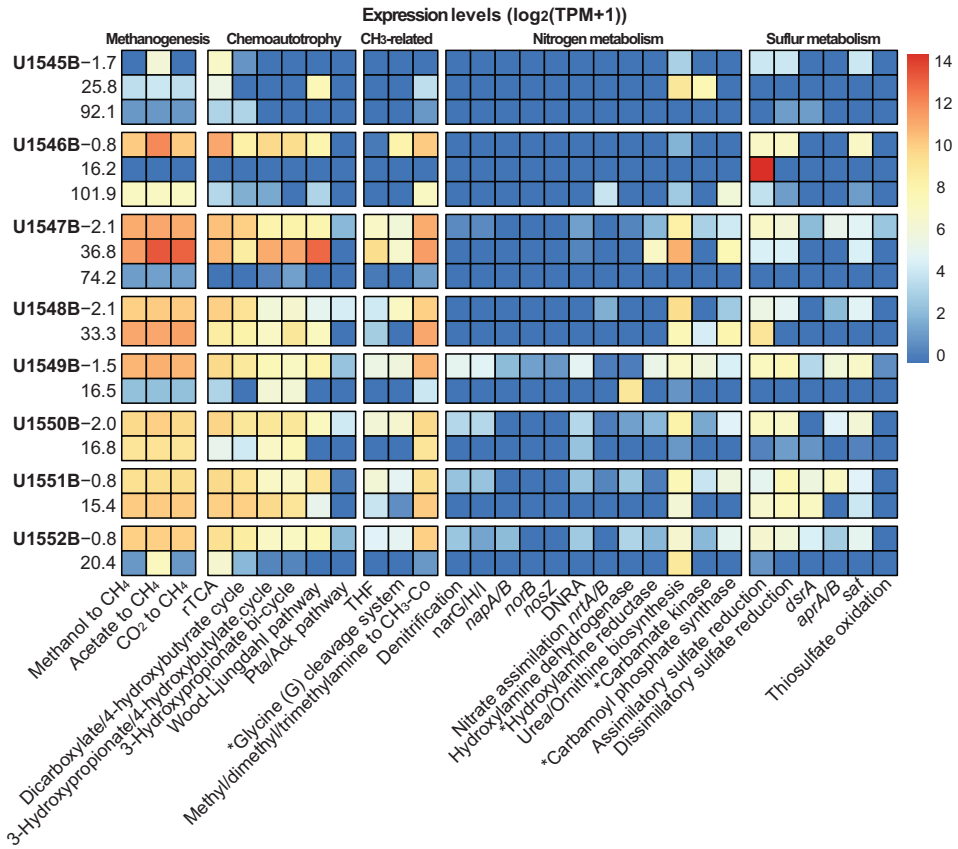

Fig. 4 Heatmap of expressed genes (log_2(TPM + 1)) associated with methanogenesis, folate and glycine biosynthesis, sulfur and nitrogen cycling, and chemoautotrophy in Guaymas Basin subsurface sediments as identified in KEGG modules. Sites and depths are along the Y axis, and depths are in meters below seafloor (mbsf). Expression levels are normalized as log_2 transformation of TPM + 1 (a value of 1 was added to TPM values to avoid zeros) (Supplementary Table 3, Source Data and "Methods"). TPM Transcripts Per Million, THF tetrahydrofolate, rTCA reductive Krebs cycle, Pta/Ack phosphate acetyltransferase/Acetate kinase, *napA/B* periplasmic nitrate reductases A/B, *narG/H/I* nitrate reductase subunits G/H/I, *norB* nitric oxide reductase, *nosZ* nitrous oxide reductase, *dsrA* dissimilatory sulfite reductase subunit A, *apr* adenylylsulfate reductase, *sat* sulfate adenylyltransferase. (*) indicates that these expressed genes were identified after manual curation of the decontaminated and non-redundant BLASTx results generated with DIAMOND against NCBI-NR database (Supplementary Table 2, Source Data and "Methods").

mRNA degradation by subsurface bacterial lineages. PNPase degrades mRNA and generates pools of ribonucleoside diphosphates (NDPs) that can support transcription performed by RNA polymerases (demonstrated under laboratory conditions; [27]). Likewise, NDPs can be converted to deoxyribonucleoside diphosphates (dNDPs) by ribonucleotide/ribonucleoside reductases [28] with the potential to be used in DNA synthesis [29]. Transcripts annotated to anaerobic, B12-dependent ribonucleotide and ribonucleoside reductases were observed in 11/19 samples, and in 10/11 samples there was co-expression with the PNPase (Fig. 6; Supplementary Table 2).

DNA and protein maintenance, degradation and repair in the Guaymas subsurface

Maintenance of DNA integrity and proteostasis are especially important for subseafloor life where elevated in situ temperatures increase the likelihood of DNA and protein damage (e.g., [30, 31]). Indeed, during manual curation of our metatranscriptomes we identified expressed genes related to DNA repair of single- and double- strand breaks, nucleotide mismatches and incision/excision nucleotide repairs, at all examined depths and sites (Fig. 6). In addition, we identified expression of DNA editing genes that initiate DNA repair upon disruptions in the genome caused by viral DNA and bacterial plasmids (e.g., CRISPR/Cas9; [32]). Alternative mechanisms for DNA repair associated with retrohoming events, (e.g., group II introns; [33]) were present in 11/19 metatranscriptomes. Evidence for uptake of exogenous DNA, for example expression of DNA competence proteins, was present at shallow depths at 6/8 sites, except for sites U1545B and U1546B (Fig. 6). DNA competence can occasionally enhance fitness through introduction of beneficial genes into genomes, or through DNA uptake as a nutrient when bacteria enter prolonged stationary growth phase (e.g., [34]).

Expressed genes with functions in proteostasis included transcripts of chaperons, chaperonins, cold shock proteins and archeases (chaperons involved in archaeal tRNA processing; [35]), and specialized archaeal heat shock chaperonins called thermosomes ([36]; Fig. 6, Supplementary Table 2). Thermosome transcripts were relatively highly expressed at all sites and were retrieved from all depths (Fig. 6). These archaeal genes were co-expressed with bacterial chaperones, suggesting both archaea and bacteria in the Guaymas subsurface invest in chaperone mediated-protein transfer and repair. We also identified expressed archaeal transcripts for specialized members of multiprotein complexes, the von Willebrand type A protein domains (vWA), which are known to promote cell adhesion and to repress cellular

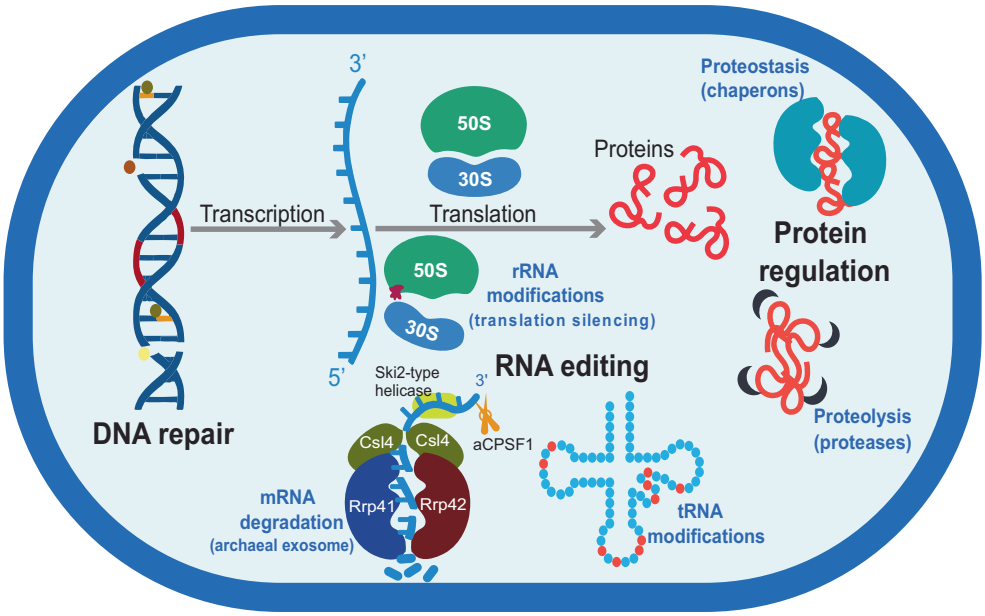

Fig. 5 Overview of expressed genes for DNA maintenance and repair, RNA editing, and protein homeostasis and degradation used by Guaymas Basin subsurface bacteria and archaea. Red, yellow and brown circles on the DNA molecule indicate expressed genes encoding DNA proteins (e.g., excinucleases, exonucleases, mismatch proteins) involved in the repair of single and double strand breaks, and mismatches (indicated with gaps, and as orange lines on the DNA molecule, respectively). Red areas on the DNA helix highlight roles of expressed genes for recombination, DNA competence and CRISPR/Cas9 editing. The red mark on the large ribosomal subunit (50 S) indicates the ribosome silencing factor that binds to the 50 S subunit and dissociates the two ribosomal subunits. The red dots on the tRNA molecule indicate positions that can be potentially modified according to the expressed genes detected in the metatranscriptomes. These modifications include thiolations (introduction of thiols in specific tRNA positions) and wobbling of tRNAs, that enables decoding of more than one synonymous mRNA codons (Supplementary Table 2).

motility ([37, 38]; Fig. 6). Such responses would benefit subsurface microorganisms that may need to adhere to localized hotspots of buried organic material, for example decaying diatoms that are infected with chytrid fungi [13]. Expression of proteases was high in almost all samples; proteasome-related enzymes (protein complexes that degrade unneeded or damaged proteins by proteolysis) were relatively highly expressed in 10/19 metatranscriptomes (Fig. 6) and were annotated to diverse archaeal taxa (Supplementary Table 2). These findings further support efficient protein repair and recycling in the hydrothermally influenced subsurface.

Persistence of circadian rhythms in the deep biosphere

Expressed transcripts encoding the archaeal circadian clock protein KaiC (histidine kinase; [39]) were identified in shallow subsurface samples (0.8–2.0 mbsf) at sites U1549B-U1552B (Fig. 3). Circadian clocks allow bacteria and archaea to adapt to oscillating environmental conditions, e.g., temperature and light [40]. In archaea, circadian clocks evolved due to primordial selection pressures (e.g., intense/mutagenic UV radiation) to ameliorate DNA-damage ("escape from light hypothesis"; [41]), and in modern archaea are suggested to regulate signal transduction processes (e.g., organization of archaellum, regulation of buoyancy using gas vesicles; [42]). Evidence of putative archaeal circadian clocks in the Guaymas hydrothermal subsurface is intriguing; nonetheless, the low expression levels of KaiC, and the detection of KaiC transcripts only in shallow sediments may reflect an evolutionary remnant whose possible effect on archaeal fitness gradually disappears in the deep biosphere.

DISCUSSION

Overall, relative expression levels of genes for metabolic processes and cellular activity in these Guaymas Basin samples are highest between 0.8 and 36.8 mbsf at all examined sites, and generally they drop to low (or near-zero) levels at depths ≥74.2 mbsf. This general pattern demonstrates rapidly declining metabolic activity of subsurface microorganisms with depth, an effect that mirrors the exponential drop in cell abundance due to temperature increase that is particularly steep at some sites (e.g., site U1547B; Fig. 2, Supplementary Table 1 and Source Data). These trends are consistent with declining 16S rRNA gene diversity for Archaea (Supplementary Fig. 1), and with downcore decreasing prokaryotic diversity based on general prokaryotic marker genes and on metagenomes (Geller-McGrath et al. under review). Downcore trends in metabolic activities may also be shaped by declining availability of labile organic matter due to long-term hydrothermal heating and increasing recalcitrance of buried organic compounds [43].

The suite of metabolic strategies detected in the metatranscriptomes expands on the metabolic capacities predicted from previous metagenomes for surficial Guaymas sediments (up to 60 cm below sea floor; [14, 15]) and from DNA microarray analyses of shallow Guaymas subsurface sediments (up to 10 mbsf; [44]). For example, expressed genes for nitrogen metabolism suggest biosynthesis of ornithine and urea is occurring in most samples (14/19; Fig. 4). This may indicate that nitrogen mineralization (e.g., ammonium production via urea) occurs at sites with different thermal and biogeochemical regimes, and possibly contributes to the elevated (up to 14 mM) ammonium concentrations detected at all examined sites (Supplementary Table 1). Nitrogen mineralization via urea was previously reported based on DNA microarray analyses only for Guaymas cold seep sediments [44]. Co-expression of carbamate kinase and carbamoyl phosphate, primarily at shallow depths where ornithine/urea biosynthesis occurs (Fig. 4), may indicate assimilation of ammonium with CO_2 or byproducts of acetogenesis (bicarbonates) into carbamyl phosphate (CP). The energy-rich CP molecule provides the carbamyl group for biosynthesis of nucleotides and ribonucleotides used for DNA and RNA synthesis, respectively [45]. Thus, the

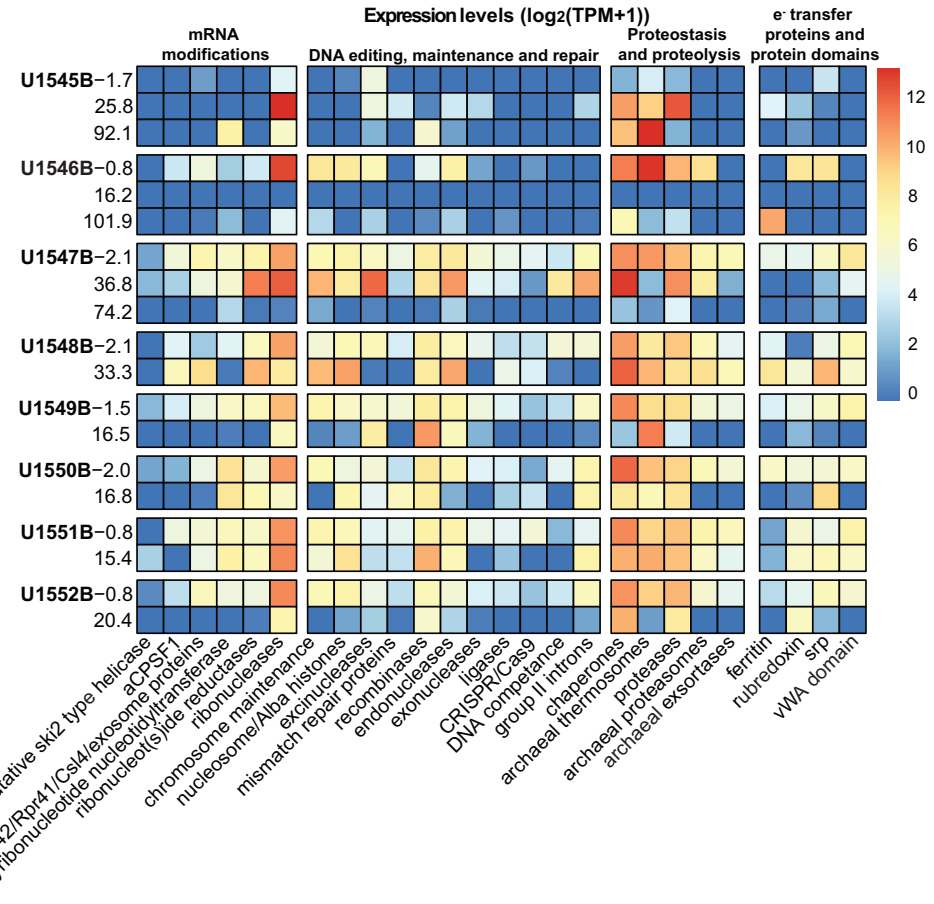

Fig. 6 Heatmap of expressed genes ($log_2(TPM + 1)$) in Guaymas Basin subsurface sediment samples associated with prokaryotic mRNA modifications, DNA maintenance and repair, proteostasis, proteolysis and electron-transfer proteins as identified with BLASTx against NR. Manual curation was performed on the decontaminated and non-redundant BLASTx results generated with DIAMOND against NCBI-NR database (Supplementary Table 2, Source Data and "Methods"). Sites and depths are along Y axis, and depths are given in meters below seafloor (mbsf). Expression levels are normalized as log_2 transformation of TPM + 1 (a value of 1 added to TPM values to avoid zeros). TPM Transcripts Per Million. vWA von Willebrand factor type A, srp signal recognition particles.

recycling of metabolic byproducts (e.g., urea, bicarbonates, CO_2) in the Guaymas subsurface could be linked to DNA/RNA (nucleotide/ribonucleotide) synthesis.

Selective aspects of RNA editing

RNA editing is a universal genome editing process that modifies all three RNA molecules (mRNA, tRNA, rRNA) and was experimentally suggested to provide adaptive advantages, and to enhance fitness in microorganisms [46]. The importance of RNA editing is evidenced by the fact that ~1% of bacterial genomes (estimate from cultured bacterial isolates) is devoted to genes involved in RNA modifications [47]. Our metatranscriptomes show that Guaymas subsurface microorganisms invest in these RNA modifications to maintain RNA homeostasis (e.g., mRNA degradation), or to reprogram RNA molecules (e.g., tRNAs) for efficient translation. Given the diverse functions these genes serve, we suggest that RNA editing and reprogramming activities identified in our data may be especially important for survival and growth of Guaymas subsurface microorganisms. As an example, near-surface sediments in Guaymas Basin, where microbial burial and subsurface entrainment begins, are rich in energy and substrates but also thermally and geochemically dynamic [48]. Dynamic environments usually demand rapid RNA editing and reprogramming for reacting quickly under changing conditions, ensuring tight translational control over cell activities [49].

The RNA modifications reported here have been described mainly under laboratory conditions and have not been elucidated in the ecological context of the deep biosphere. As an example, expressed genes associated with tRNA thiolations are known to control translational fidelity in bacterial and yeast isolates, and to coordinate the availability of sulfur-containing amino acids when nutrients become scarce [50]. Likewise, transcripts associated with tRNA wobbling were experimentally shown to facilitate maintenance of cellular homeostasis under stationary-phase conditions, and adaptation to nutrient limitation [51]. In our dataset, relatively high expression levels of diverse tRNA modification genes are detected at all sites between 0.8 and 36.8 mbsf. Over the first 50 mbsf, temperatures can increase significantly from 14-18°C (~2 mbsf) to 40-50°C at ~50 mbsf (especially at hot Ringvent sites; Supplementary Table 1; Fig. 2, [52]). Steep biogeochemical gradients are changing the sedimentary habitat; for example, active dissimilatory sulfate reduction is depleting sulfate and produces sulfide (Supplementary Table 1). Along these thermal and biogeochemical gradients, tRNA editing could be especially important for supporting survival by efficiently coordinating housekeeping processes like translation, and amino acid availability as in situ conditions change. Similarly, transcripts annotated to the ribosomal silencing factor can also increase chances of survival under unfavorable conditions by provoking translational arrest via ribosomal disassociation, under elevated temperatures or energy limitation (e.g., [53]).

Overall, tRNA modifications and ribosomal silencing would be beneficial responses to substrate and nutrient limitation and temperature increase in Guaymas Basin. These modifications can

facilitate the transition from more active microorganisms in surficial and shallow/intermediate subsurface sediments (e.g., [13, 16], this study), to less active microorganisms in deeper subsurface realms where sulfide concentrations and temperature can increase drastically, and nutrients and energy sources likely become limiting. Some taxa, less adapted to in situ subsurface conditions, may need to pause their translation or slow their growth when conditions become unfavorable. In fact, we observe expression of these ribosomal silencing factor genes in greatest abundance at Ringvent site U1547B at 36.8 mbsf where in situ temperature reaches 31.8°C, and sulfide concentrations increase 1000-fold relative to shallow depths (Supplementary Table 1). In sum, ribosomal silencing could be a "last minute escape button" for subsurface microorganisms that must transition to a dormant state for survival. The ability to efficiently modulate growth and (temporarily) transition to a dormant state for survival, is likely one factor that selects bacteria and archaea from surficial sediment communities that can survive in the deep biosphere [54, 55].

mRNA degradation and nucleotide recycling

In the Guaymas subsurface cell counts drop drastically below 50 mbsf (Fig. 2) and with increasing temperature and depth, cells may walk a fine line between utilizing strategies that salvage critical nutrients to remain active, vs. entering stationary-phase, long-term dormancy (e.g., spore formation), or cell death. Prokaryotes orchestrate mRNA degradation in response to various environmental cues including amino acid starvation, DNA damage and heat shock [56]. Degraded mRNA products (NDPs) may be salvaged and used as nutrients or as structural subunits in DNA replication. Microbial consumption of nucleic acids (DNA) is demonstrated to increase competitive fitness when cells enter long-term stationary phase [57]. Experimental evidence indicates that dNDPs support DNA synthesis if nutrients required for de novo nucleotide synthesis are in short supply [29]. We observe expression of genes for mRNA degradation performed by a suite of enzymes annotated to archaea and bacteria primarily at shallow/intermediate depths of sites U1547B-U1552B (0.8-36.8 mbsf). At Ringvent sites U1547B and U1548B we observe increasing relative expression of genes for ribonucleotide/ribonucleoside reductases with depth that can potentially convert dNDPs to triphosphorylated substrates (dNTPs) (highest expression at 74.2 mbsf at U1547B; Fig. 6). Nucleotide synthesis by this process would proceed at slower rates, due to the higher activation energy of dNDPs compared to dNTPs [29]. Resulting slow rates of DNA synthesis would be consistent with predicted long doubling times of subsurface microorganisms, especially at depths where energy is limited (e.g., [58, 59]). At hotter sites (e.g., Ringvent sites where temperatures can exceed 50°C) the energy penalty of using dNDPs could be less prohibitive because high temperature can lower the activation energy required for thermostable DNA polymerases to utilize dNDPs over dNTPs [29]. Overall, dNDP recycling can be energetically less costly than de novo synthesis, and the most promising strategy for heat-stressed cells that must conserve energy for other processes including repair of damaged DNA and proteins.

Costs of RNA editing

The fractional cost (relative to the total cellular energy budget) of maintaining transcription, translation and protein assembly in non-dormant cells is estimated to be one to two orders of magnitude higher compared to the cost of genome/DNA maintenance [60]. Despite the putative energy barriers anticipated to exist in the deep biosphere (e.g., decreasing energy fluxes with depth; [58]), we find evidence for microorganisms in the Guaymas Basin subsurface, at least up to 101.9 mbsf, that actively express a repertoire of RNA modifications that may enhance survival. A portion of the energetic cost of these RNA modifications could be paid for via fine-tuned recycling and salvage of RNA. Certain RNA modifications that we report (e.g., mRNA degradation, thiolation and wobbling of tRNAs), as well as conserved chromatin (de)acetylases, primarily annotated to Bathyarchaeota (e.g., Alba proteins linked with RNA metabolism; [61]), are thought to be traceable to a last universal common ancestor (LUCA) [62, 63]. These modifications are known to be successful strategies for conserving energy by regulating carbon and nitrogen homeostasis [64], helping cells to adapt to extreme temperatures, and by controlling micronutrient (e.g., iron/phosphate) acquisition (e.g., [65–67]). Aside from stress-related adaptations, RNA editing can also confer immunity against viral and bacterial attacks. It is suggested that tRNA modifications in archaea provide immunity against archaeal viruses that use tRNA genes as integration targets [68]. Viral activity in the deep biosphere and in hydrothermal vent systems is known (e.g., [69–71]) and viral transcripts, which require future examination, were recovered within our metatranscriptomes.

Archaeal signaling in the subsurface

Manually identified transcripts for chromosome segregation and sporulation proteins (Figs. 3, 6; Supplementary Table 2) indicate that the Guaymas subsurface hosts a mixed community of active and dormant microorganisms. In non-photosynthetic prokaryotes cell fate decisions associated with growth vs. sporulation and oxidative stress responses (e.g., expression/translation of Fe-S cluster rubredoxins and ferredoxins) are thought to be controlled by timekeeping mechanisms like circadian clocks [42, 72–74]. We observe that expressed archaeal rubredoxin and ferredoxin genes (annotated primarily to Lokiarchaeota and Thermoplasmata), signal recognition particles (associated with protein trafficking, and annotated to Lokiarchaeota, Heimdallarchaeota, Bathyarchaeota, Thermoplasmata) and archaeal flagellin (annotated to Thermoplasmatales) are often co-expressed with the archaeal KaiC kinase (Figs. 3, 6; Supplementary Table 2). KaiC kinases are suggested to regulate complex signaling networks involved in motility and oxidative stress responses in archaea [42], and may play similar roles in the shallow Guaymas subsurface (0.8–2.0 mbsf; U1549-U1552B). Considering the overall low expression of KaiC in our metatranscriptomes, this hypothesis will require future examination using genetic manipulation of cultured Guaymas archaeal isolates. We also note that bacterial rubredoxins and ferredoxins in our datasets (annotated primarily to Chloroflexi, Atribacteria and Desulfobacterota) can also participate as electron carriers in other processes aside from oxidative stress responses, including *n*-alkane mineralization and iron reduction/sulfur sequestration [75, 76]. These processes are likely relevant in the Guaymas subsurface where abundant iron [77], *n*-alkanes (Supplementary Table 5), and sulfur (Supplementary Table 1) concentrations are found.

Range and limitations of protein maintenance

Incubations of sediments from the Nankai Trough subduction zone (IODP370 > 200 mbsf heated to ~120 °C) with sulfur and carbon radiotracers suggested that protein repair occurs at an essential energetic cost that can be covered by rapid substrate turnover [31]; however, no genomic or metatranscriptomic data are available for those deep and extremely hot samples retrieved from Nankai Trough. While our mRNA data were obtained from sediments at maximum depths of 101.9 mbsf and temperatures up to 51°C, within this range, active microorganisms also express a suite of molecular chaperons at all examined sites, which help to maintain and repair active proteins at the expense of ATP. The relative expression of chaperons generally increased with depth, particularly at the hot Ringvent sites, except for one Ringvent sample at 74.2 mbsf (U1547B), where cell counts drop down to ~10^4 cells per cm^{-3} of sediment (Fig. 2). Actively dividing cells are more prone to spontaneous protein misfolding and protein aggregation compared to stationary cells where errors of folding

may be rarer [78]. Although protein repair is energetically demanding, prolonged accumulation of misfolded proteins jeopardizes cellular homeostasis, which explains the evolutionary retention of energetically expensive protein repair processes [78]. Overall, the cost of chaperone-mediated repair is significantly lower than the cost of protein degradation and de novo resynthesis [79], and this relative efficiency of repair can offset some of the cost explaining the variety of different chaperons identified in our samples (Supplementary Table 2).

CONCLUSION

Prokaryotic activity and gene expression in the Guaymas Basin subsurface are not maintained by extremophiles that are fundamentally different from other microorganisms. This study on expressed genes by Guaymas subsurface microorganisms from sites and depths with contrasting biogeochemistry and temperature profiles, indicates that some fraction of the subsurface prokaryotic community is active, and that many/most of these taxa must be efficient recyclers that struggle to survive and access sufficient resources for their maintenance and growth. With increased burial, these populations at any given time are likely balancing the capacity for activity with inevitable periods of dormancy or even death. Aside from the use of metabolic strategies for obtaining carbon and energy, previously associated with deep biosphere (e.g., chemoautotrophy, methane, and sulfur cycling), survival in the Guaymas subsurface is also facilitated by mechanisms that permit fine-tuning of cellular activities that include RNA editing, ribosomal silencing, and protein homeostasis. These processes collectively help diverse bacterial and archaeal lineages to succeed/persist in this challenging habitat.

METHODS

Sample collection

International Ocean Discovery Program Expedition 385 (IODP 385) drilled organic-rich sediments and intruded sills in the off-axis region, and the northern axial graben of Guaymas Basin during a 90-days expedition between September and November 2019 [52]. Among the major objectives of IODP 385 was to examine the subsurface biosphere of Guaymas Basin and investigate microbial responses and adaptations under the different sill-driven hydrothermal conditions that occur in the broader region of the Basin. Sill intrusions in Guaymas Basin extend tens of kilometers off axis and provide transient heat that drives hydrothermal circulation in the sediments of the basin, and mobilizes buried sedimentary carbon [52]. The thermal and geochemical gradients that emerge from this circulation shape the abundance, composition, and activity of the deep subsurface biosphere of the basin.

IODP 385 drilled eight sites (U1545-U1552 thereafter referred as U1545B-U1552B to indicate also the hole -B- devoted for microbiology samples) with different thermal and geochemical regimes, and differences in the depths and thickness of sill intrusions present in the sediments. The drilling sites included (a) the adjacent sites U1545B and U1546B located ~52 km northwest of the northern Guaymas Basin axial trough, (b) the hydrothermal sites U1547B and U1548B ~ 27 km northwest of the axial trough, (c) the two cold seep sites U1549B and U1552B found off-axis, (d) site U1550B at the northern axial valley and (e) site U1551B ~ 29 km southeast of the axial trough ([52]; Fig. 1, Table 1). Drilling sites U1545B and U1546B recovered sediments from ~390 meters below seafloor (mbsf). U1546B has a massive sill below ~350 mbsf that affects the surrounding sediment; the temperature range at both U1546B and U1545B spanned from cold-seafloor temperatures (~5 °C) to hot (~60 °C) subsurface sediments (~240 mbsf) covering a thermal gradient suitable for growth of psychrophilic mesophilic and thermophilic microorganisms. Sites U1547B and U1548B (Ringvent sites; drilled down to ~210 mbsf) are sites with active hydrothermal systems and thick sills at a shallow depth (~ 99 mbsf and below). The temperatures at Ringvent increase sharply below 8 mbsf (~ 17°C), reaching ~50°C at 74 mbsf and 96°C at 150 mbsf. Cold seep site U1549B and site U1552B drilled near a methane hydrate area, are located ~9.5 km and 20 km northwest of the northern axial trough of Guaymas Basin, respectively. U1552 site is described to produce massive amounts of gas hydrates [52]. Finally, site 1550B is documented to have great hydrocarbon formation near the sill/sediment contact and site U1551B to receive terrigenous inputs.

Sediment cores were collected using the drilling vessel *JOIDES Resolution*. Holes were first advanced using advanced piston coring (APC), then half-length APC, and then extended core barrel (XCB) coring as necessary. Temperature measurements were made using the advanced piston corer temperature (APCT-3) and Sediment Temperature 2 (SET2) tools. After coring, downhole logging used the triple combination and Formation MicroScanner sonic logging tool strings. After bringing core sections onto the core receiving platform of the D/V *JOIDES Resolution*, sampling for RNA occurred immediately after core retrieval on the core receiving platform by sub-coring with a sterile, cutoff 50cc syringe into the center of each freshly cut core section targeted. These sub-cores were immediately frozen in liquid nitrogen and stored at −80 °C.

For DNA-based studies, whole round sections were immediately transferred (within 30 min) to the laboratory after placing them in gas-tight sterile bags. Masks, gloves and laboratory coats were worn during sample handling in the laboratory where core samples were transferred from their gas-tight bags onto sterilized foil on the bench surface inside a Table KOACH T 500-F system, which creates an ISO Class I clean air environment (Koken Ltd., Japan). In addition, the bench surface was targeted with a fanless ionizer (Winstat BF2MA, Shishido Electrostatic Co., Ltd., Japan) for neutralizing static charge on the surface of working materials especially plasticware to avoid contamination by electrostatic attraction. Within this clean space, the exterior 2 cm of each extruded section was removed using a sterilized ceramic knife. The core interior was transferred to sterile 50-mL Falcon tubes, labeled, and immediately frozen at −80 °C for post cruise analyses.

RNA isolation, and metatranscriptome library preparation, and analysis

RNA extraction and sequencing. Total RNA was extracted successfully from 19 sediment samples from sites U1545B-U1552B (Supplementary Table 1). Before each RNA extraction, all samples including a blank sample (control), were washed twice with absolute ethanol (200 proof; purity ≥ 99.5%; Thermo Scientific Chemicals), and one time with DEPC water (Fisher BioReagents) to remove hydrocarbons and other inhibitory elements present in Guyamas sediments, that without these washes, resulted in low or zero RNA yield. In brief, 13–15g of frozen sediments were transferred into UV-sterilized 50 ml Falcon tubes (RNAase/DNase free) using clean, autoclaved and ethanol-washed metallic spatulas. Each tube received an equal volume of absolute ethanol and was shaken manually for 2 min followed by 30 s of vortexing at full speed to create a slurry. Samples were transferred into an Eppendorf centrifuge (5810 R) and were centrifuged at room temperature for 2 min at 2000 rpm. The supernatant was decanted, and the ethanol wash was repeated. After decanting the supernatant of the second ethanol wash, an equal volume of DEPC water was added into each sample. Samples were manually shaken and vortexed as before to create slurry, and were transferred into the Eppendorf centrifuge (5810 R) where they were centrifuged at room temperature for 2 min at 2000 rpm. The supernatant was decanted, and each sediment sample was immediately divided into three bead-containing 15 mL Falcon tubes, provided by the PowerSoil Total RNA Isolation Kit (Qiagen). RNA was extracted as suggested by the manufacturer with the modification that the RNA extracted from the three aliquots was pooled into one RNA collection column and eluted at 30 µl final volume. All RNA extractions were performed in a UV-sterilized clean hood (two UV cycles of 15 min each) that was installed with HEPA filters. Surfaces inside the hood and pipettes were thoroughly cleaned with RNase AWAY (Thermo Scientific) before every RNA extraction and in between extraction steps. Trace DNA contaminants were removed from RNA extracts using TURBO Dnase (Thermo Fisher Scientific) and the manufacturer's protocol. Removal of DNA from the RNA extracts was confirmed with PCR reactions using the bacterial primers BACT1369F/PROK1541R (F: 5′CGGTGAATACGTTCYCGG 3′, R: 5′AAGGAGGTGATCCRGCCGCA 3′; [80]), targeting the small ribosomal subunit (SSU) of 16S rRNA gene. Each 25 µl PCR reaction was prepared using GoTaq G2 Flexi DNA Polymerase (Promega) and contained 0.5 U μl^{-1} GoTaq G2 Flexi DNA Polymerase, 1X Colorless GoTaq Flexi Buffer, 2.5 mM $MgCl_2$, (Promega) 0.4 mM dNTP Mix (Promega), 4 µM of each primer (final concentrations), and DEPC water. These PCR amplifications were performed in an Eppendorf Mastercycler Pro S Vapoprotect (Model 6321) thermocycler with following conditions: 94 °C for 5 min, followed by 35 cycles of 94 °C (30 s), 55 °C (30 s), and 72 °C (45 s). The PCR reaction

products were run in 2% agarose gels (Low-EEO/Multi-Purpose/Molecular Biology Grade Fisher BioReagents) to confirm absence of DNA products. RNA quantification (ng μl^{-1}) was performed using Qubit RNA High Sensitivity (HS), Broad Range (BR), and Extended Range (XR) Assay Kits, (Invitrogen).

Amplified cDNAs from the DNA-free RNA extracts were prepared using the Ovation RNA-Seq System V2 (Tecan) following manufacturer's suggestions. cDNAs were submitted to the Georgia Genomics and Bioinformatics Core for library preparation and sequencing using NextSeq 500 PE 150 High Output (Illumina). The sequencing of the cDNA library from the control sample was unsuccessful as it failed to generate any sequences that met the length criterion of 300-400 base pairs.

Metatranscriptome data analyses. Raw sequencing reads were trimmed to remove adapters and low-quality bases using *fastp* (v0.23.2) [81] with parameters (-q 20 -u 20 -l 50 -w 16 -5 -M 30 -g -D --detect_adapter_for_pe --dup_calc_accuracy 6). We used Trinity (v2.14.0) [82] to assemble the 19 metatranscriptomes with default settings. Trinity generated 640,136 assembled metatranscripts with size > 165 bp. We performed DIAMOND (v.2.0.7) BLASTx [83] against NCBI-NR database (release date: 2022-12-04) to provide functional and taxonomic annotations on the assembled metatranscriptomes. Because the control sample failed to generate sequences that met the minimum length criterion, the annotated transcripts with e-values > 1e−5 were manually curated to remove possible contaminants by creating an in-house database that contained putative contaminant species (taxa identified as potential kit contaminants and human pathogens; e.g., [84]). Taxa used in the in-house database are provided in Supplementary Table 6. Transcripts with > 90% similarity to the in-house database over >50% of contig length were removed for downstream analyses. This process removed 8,301 transcripts (8,301/640,136; ~1.2%). The remaining decontaminated assembled transcripts were processed with Prodigal (v2.6.3; [85]) to predict gene and protein sequences. CD-hit [86] (v. 4.8.1; -c 0.95 -aS 0.9 -n 10) was used to cluster genes and to remove redundancy. For functional annotation, KofamScan (v.1.3.0) [87] and GhostKOALA (v.2.2) [88] were used to assign orthologs (KOs) to protein sequences using the Kyoto Encyclopedia of Genes and Genomes (KEGG) database. DIAMOND (v.2.0.7) BLASTp [83] (v2.0.15.153, -e 1e−5 --more-sensitive) was used to search against NCBI-NR database (release date: 2022-12-04).

To gain a more detailed insight on the function and taxonomy of the expressed genes, the decontaminated and non-redundant assembled transcripts were re-run with DIAMOND BLASTx [83] (v2.0.15.153, -e 1e−5 --more-sensitive) against NCBI-NR database (release date: 2022-12-04). The BLASTx results with e-values > 1e−5 were manually curated for expression of genes involved in methane, nitrogen, sulfur and folate metabolisms, carbon fixation, C1 from folate, glycine cleavage system, DNA maintenance and repair, RNA modifications, proteostasis, proteolysis, arsenic detoxification, cadmium and copper transport, tungsten-containing aldehyde ferredoxin oxidoreductases, circadian rhythm, ferredoxins, rubredoxins, signal recognition particle protein, archaeal flagellin, von Willebrand type A domains, sporulation, Ni-Fe hydrogenases, haloacid reductive dehalogenases (see also Supplementary Table 2). We recognize that any automated and manual pipeline that is used to assign gene function has the caveat that publicly available databases may contain some protein sequences that have not been functionally validated on the bench.

The expression level of each transcript was estimated in units of transcripts per million (TPM) using Salmon (v1.9.0, --meta) [89]. The TPM values of all transcripts annotated to same gene were summed and were added to a value of 1 (to avoid zeros) and normalized using log_2-transformation. Metatranscriptome reads were deposited to the National Center for Biotechnology Information Sequence Read Archive under accession numbers SRR22580929-SRR22580947.

Archaeal 16S rRNA marker gene analyses

DNA was extracted from all 8 sites and at depths between 0.8 to 177.4 mbsf using a FastDNA SPIN Kit for Soil (MP Biomedicals) following the manufacturer's protocol. The DNA was PCR-amplified using the archaeal primers Arch25F (5'TCYGKTTGATCCYGSCRG 3'; [90]) and Arch806R (5'GGACTACVSGGGTATCTAAT 3'; [91]) targeting ~800 base pairs (bp) between the V2-V4 regions of the archaeal 16SrRNA SSU. PCR amplifications were performed using the SpeedSTAR HS DNA Polymerase (TAKARA) kit with the following modifications: each 25 µl PCR reaction contained up to 1 ng of template DNA, 2X Fast Buffer I, 2.5 mM dNTP mixture, 5 units of SpeedSTAR HS DNA Polymerase, 10 mM of each primer and DEPC water (Fisher BioReagents). The PCR amplifications were performed in an Eppendorf Mastercycler Pro S Vapoprotect (Model 6321) thermocycler with the following conditions: 95 °C for 5 min, followed by 30 cycles of 94 °C (30 s), 55 °C (30 s), 72 °C (45 s). The total volume of PCR reactions was run in 2% agarose gel (Low-EEO/Multi-Purpose/Molecular Biology Grade Fisher BioReagents) and the correct size PCR products (~800 bp), were isolated and recovered from the gel using the Zymoclean Gel DNA Recovery Kit as instructed by the manufacturer. Libraries for DNA PacBio sequencing (long-read sequencing) were prepared from the recovered and gel purified DNA extracts at the University of Delaware DNA Sequencing & Genotyping Center.

The generated PacBio sequences were analyzed using QIIME2 (v.2022.8) [92] pipeline for single-end generated sequences. Dada2 denoise-ccs plugin provided in the QIIME2 pipeline was used to denoise, dereplicate and filter out chimera reads. Taxonomy was assigned to amplicon sequence variants (ASVs) using the scikit-learn multinomial naïve Bayes classifier (q2-feature-classifier plugin; [93]) with the SILVA database (v138.1) as reference database [94]. PacBio reads were deposited to the National Center for Biotechnology Information Sequence Read Archive under access numbers SRR23604162-SRR23604206.

Cell counts

The sediment sampling for cell counts occurred immediately after core retrieval on the core receiving platform by sub-coring with a sterile, tip-cut 2.5 cc syringe from the center of each freshly cut core section. Approximately 2 cm^3 sub-cores were immediately put into tubes containing fixation solution consisting of 8 mL of 3xPBS (Gibco PBS, pH 7.4, Fischer) and 5% (v/v) neutralized formalin (Thermo Scientific Shandon Formal-Fixx Neutral Buffered Formalin). If necessary, the mixture was stored at 4 °C.

Fixed cells were separated from the slurry using ultrasonication and density gradient centrifugation [95]. For cell detachment, a 1 ml aliquot of the formalin-fixed sediment slurry was amended with 1.4 ml of 2.5% NaCl, 300 µl of pure methanol, and 300 µl of detergent mix ([96]; 100 mM ethylenediamine tetraacetic acid [EDTA], 100 mM sodium pyrophosphate, 1% [v/v] Tween-80). The mixture was thoroughly shaken for 60 min (Shake Master, Bio Medical Science, Japan), and subsequently sonicated at 160 W for 30 s for 10 cycles (Bioruptor UCD-250HSA; Cosmo Bio, Japan). The detached cells were recovered by centrifugation based on the density difference of microbial cells and sediment particles, which allows collection of microbial cells in a low-density layer. The sample was transferred onto a set of four density layers composed of 30% Nycodenz (1.15 g $cm–^3$), 50% Nycodenz (1.25 g cm^{-3}), 80% Nycodenz (1.42 g cm^{-3}), and 67% sodium polytungstate (2.08 g cm^{-3}). Cells and sediment particles were separated by centrifugation at 10,000 × g for 1 h at 25 °C. The light density layer was collected using a 20 G needle syringe. The heavy fraction, including precipitated sediment particles, was resuspended with 5 mL of 2.5% NaCl, and centrifuged at 5000 × *g* for 15 min at 25 °C. The supernatant was combined with the previously recovered light density fraction. With the remaining sediment pellet, the density separation was repeated. The sediment was resuspended using 2.1 ml of 2.5% NaCl, 300 µl of methanol, and 300 µl of detergent mix and shaken at 500 rpm for 60 min at 25 °C, before the slurry sample was transferred into a fresh centrifugation tube where it was layered onto another density gradient and separated by centrifugation just as before. The light density layer was collected using a 20 G needle syringe, and combined with the previously collected light density fraction and supernatant to form a single suspension for cell counting.

For cell enumeration, a 50%-aliquot of the collected cell suspension was passed through a 0.22-µm polycarbonate membrane filter. Cells on the membrane filter were treated with SYBR Green I nucleic acid staining solution (1/40 of the stock concentration of SYBR Green I diluted in Tris-EDTA [TE] buffer). The number of SYBR Green I– stained cells were enumerated either by a direct microscopic count [97] or an image-based discriminative count [98]. For image-based discriminative counting, the Count Nuclei function of the MetaMorph software (Molecular Devices) was used to detect and enumerate microbial cells.

DATA AVAILABILITY

The raw metatranscriptome sequencing data in this study have been deposited in the National Center for Biotechnology Information Sequence Read Archive under the accession numbers SRR22580929-SRR22580947. PacBio reads were deposited to the

National Center for Biotechnology Information Sequence Read Archive under access numbers SRR23604162-SRR23604206.

CODE AVAILABILITY

The custom R scripts used in this study are publicly available at Zenodo (https://doi.org/10.5281/zenodo.7710615) [99].

REFERENCES

1. Dick GJ. The microbiomes of deep-sea hydrothermal vents: distributed globally, shaped locally. Nat Rev Microbiol. 2019;17:271–83.
2. Lanzén A, Jørgensen SL, Bengtsson MM, Jonassen I, Øvreås L, Urich T. Exploring the composition and diversity of microbial communities at the Jan Mayen hydrothermal vent field using RNA and DNA. FEMS Microbiol Ecol. 2011;77:577–89.
3. Biddle JF, Cardman Z, Mendlovitz H, Albert DB, Lloyd KG, Boetius A, et al. Anaerobic oxidation of methane at different temperature regimes in Guaymas Basin hydrothermal sediments. ISME J. 2012;6:1018–31.
4. Lesniewski R, Jain S, Anantharaman K, Schloss PD, Dick GJ. The metatranscriptome of a deep-sea hydrothermal plume is dominated by water column methanotrophs and lithotrophs. ISME J. 2012;6:2257–68.
5. Urich T, Lanzén A, Stokke R, Pedersen RB, Bayer C, Thorseth IH, et al. Microbial community structure and functioning in marine sediments associated with diffuse hydrothermal venting assessed by integrated meta-omics. Environ Microbiol. 2014;16:2699–710.
6. Stokke R, Dahle H, Roalkvam I, Wissuwa J, Daae FL, Tooming-Klunderud A, et al. Functional interactions among filamentous Epsilonproteobacteria and bacteroidetes in a deep-sea hydrothermal vent biofilm. Environ Microbiol 2015;17:4063–77.
7. Fortunato CS, Butterfield DA, Larson B, Lawrence-Slavas N, Algar CK, Zeigler Allen L, et al. Seafloor incubation experiment with deep-sea hydrothermal vent fluid reveals effect of pressure and lag time on autotrophic microbial communities. Appl Environ Microbiol. 2021;87:e00078–21.
8. Fortunato C, Huber J. Coupled RNA-SIP and metatranscriptomics of active chemolithoautotrophic communities at a deep-sea hydrothermal vent. ISME J. 2016;10:1925–38.
9. Lonsdale P, Becker K. Hydrothermal plumes, hot springs, and conductive heat flow in the Southern Trough of Guaymas Basin. Earth Planet Sci Lett 1985;73:211–25.
10. Von Damm KL, Edmond JM, Measures CI, Grant B. Chemistry of submarine hydrothermal solutions at Guaymas Basin, Gulf of California. Geochim Cosmochim Acta. 1985;49:2221–37.
11. Simoneit BRT, Schoell M. Carbon isotope systematics of individual hydrocarbons in hydrothermal petroleums from the Guaymas Basin, Gulf of California. Org Geochem 1995;23:857–63.
12. Cruaud P, Vigneron A, Pignet P, Caprais J-C, Lesongeur F, Toffin L, et al. Comparative study of Guaymas Basin microbiomes: cold seeps vs. hydrothermal vents sediments. Front Mar Sci 2015;4:417.
13. Ramírez GA, Mara P, Sehein T, Wegener G, Chambers CR, Joye SB, et al. Environmental factors shaping bacterial, archaeal and fungal community structure in hydrothermal sediments of Guaymas Basin, Gulf of California. PLoS One. 2021;16:e0256321.
14. Dombrowski N, Teske AP, Baker BJ. Expansive microbial metabolic versatility and biodiversity in dynamic Guaymas Basin hydrothermal sediments. Nat Commun. 2018;9:4999.
15. Seitz KW, Dombrowski N, Eme L, Spang A, Lombard J, Sieber JR, et al. Asgard archaea capable of anaerobic hydrocarbon cycling. Nat Commun. 2019;10:1822.
16. Ramírez GA, McKay LJ, Fields MW, Buckley A, Mortera C, Hensen C, et al. The Guaymas Basin subseafloor sedimentary archaeome reflects complex environmental histories. iScience. 2020;23:101459.
17. Lizarralde D, Teske A, Höfig TW, González-Fernández A, the IODP Expedition 385 Scientists. Carbon release by sill intrusion into young sediments measured through scientific drilling. Geology. 2023;51:329–33.
18. Kikuchi G, Motokawa Y, Yoshida T, Hiraga K. Glycine cleavage system: reaction mechanism, physiological significance, and hyperglycinemia. Proc Jpn Acad Ser B Phys Biol Sci. 2008;84:246–63.
19. Price MN, Deutschbauer AM, Arkin AP. Four families of folate-independent methionine synthases. PLoS Genet. 2021;17:e1009342.
20. Danchin A, Sekowska A, You C. One-carbon metabolism, folate, zinc and translation. Micro Biotechnol. 2020;13:899–925.
21. Büttner K, Wenig K, Hopfner KP. Structural framework for the mechanism of archaeal exosomes in RNA processing. Mol Cell. 2005;20:461–71.
22. Johnson SJ, Jackson RN. Ski2-like RNA helicase structures: common themes and complex assemblies. RNA Biol. 2013;10:33–43.
23. Clouet-d'Orval B, Phung DK, Langendijk-Genevaux PS, Quentin Y. Universal RNA-degrading enzymes in Archaea: Prevalence, activities and functions of β-CASP ribonucleases. Biochimie. 2015;118:278–85.
24. Cousineau B, Smith D, Lawrence-Cavanagh S, Mueller JE, Yang J, Mills D, et al. Retrohoming of a bacterial group II intron: mobility via complete reverse splicing, independent of homologous DNA recombination. Cell. 1995;94:451–62.
25. Evguenieva-Hackenberg, E The archaeal exosome. in *RNA Exosome. Advances in Experimental Medicine and Biology* (eds Jensen, TH) 29–38 (Springer, New York, 2010).
26. Cameron TA, Matz LM, De Lay NR. Polynucleotide phosphorylase: Not merely an RNase but a pivotal post-transcriptional regulator. PLoS Genet. 2018;14:e1007654.
27. Gottesman ME, Mustaev A. Ribonucleoside-5′-diphosphates (NDPs) support RNA polymerase transcription, suggesting NDPs may have been substrates for primordial nucleic acid biosynthesis. J Biol Chem. 2019;294:11785–92.
28. Guzmán EC, Caballero JL, Jiménez-Sánchez A. Ribonucleoside diphosphate reductase is a component of the replication hyperstructure in *Escherichia coli*. Mol Microbiol. 2002;43:487–95.
29. Burke CR, Lupták A. DNA synthesis from diphosphate substrates by DNA polymerases. Proc Natl Acad Sci USA. 2018;115:980–5.
30. Orsi WD, Edgcomb VP, Christman GD, Biddle JF. Gene expression in the deep biosphere. Nature. 2013;499:205–8.
31. Beulig F, Schubert F, Adhikari RR, Glombitza C, Heuer VB, Hinrichs KU, et al. Rapid metabolism fosters microbial survival in the deep, hot subseafloor biosphere. Nat Commun. 2022;13:312.
32. Rath D, Amlinger L, Rath A, Lundgren M. The CRISPR-Cas immune system: biology, mechanisms and applications. Biochimie. 2015;117:119–28.
33. Matsuura M. A bacterial group II intron encoding reverse transcriptase, maturase, and DNA endonuclease activities. Genes Dev. 1997;11:2910–24.
34. Palchevskiy V, Finkel SE. Escherichia coli competence gene homologs are essential for competitive fitness and the use of DNA as a nutrient. J Bacteriol. 2006;188:3902–10.
35. Auxilien S, El Khadali F, Rasmussen A, Douthwaite S, Grosjean H. Archease from Pyrococcus abyssi improves substrate specificity and solubility of a tRNA m5C methyltransferase. J Biol Chem. 2007;282:18711–21.
36. Klumpp M, Baumeister W. The thermosome: archetype of group II chaperonins. FEBS Lett. 1998;430:73–7.
37. Whittaker CA, Hynes RO. Distribution and evolution of von Willebrand/integrin A domains: widely dispersed domains with roles in cell adhesion and elsewhere. Mol Biol Cell. 2002;13:3369–87.
38. Hoffmann L, Anders K, Bischof LF, Ye X, Reimann J, Khadouma S, et al. Structure and interactions of the archaeal motility repression module ArnA-ArnB that modulates archaellum gene expression in *Sulfolobus acidocaldarius*. J Biol Chem. 2019;294:7460–71.
39. Schmelling NM, Lehmann R, Chaudhury P, Beck C, Albers SV, Axmann IM, et al. Minimal tool set for a prokaryotic circadian clock. BMC Evol Biol. 2017;17:169.
40. Jabbur ML, Johnson CH. Spectres of clock evolution: past, present, and yet to come. Front Physiol. 2022;12:815847.
41. Rosato E, Kyriacou CP. Origins of circadian rhythmicity. J Biol Rhythms. 2002;17:506–11.
42. Makarova KS, Galperin MY, Koonin EV. Proposed role for KaiC-like ATPases as major signal transduction hubs in Archaea. mBio. 2017;8:e01959–17.
43. Lin YS, Koch BP, Feseker T, Ziervogel K, Goldhammer T, Schmidt F, et al. Near-surface heating of young rift sediment causes mass production and discharge of reactive dissolved organic matter. Sci Rep. 2017;7:44864.
44. Vigneron A, Cruaud P, Roussel EG, Pignet P, Caprais JC, Callac N, et al. Phylogenetic and functional diversity of microbial communities associated with subsurface sediments of the Sonora Margin, Guaymas Basin. PLoS One. 2014;9:e104427.
45. Jones ME. Carbamyl Phosphate: Many forms of life use this molecule to synthesize arginine, uracil, and adenosine triphosphate. Science. 1963;140:1373–9.
46. Xin K, Zhang Y, Fan L, Qi Z, Feng C, Wang Q, et al. Experimental evidence for the functional importance and adaptive advantage of A-to-I RNA editing in fungi. Proc Natl Acad Sci USA. 2023;120:e2219029120.
47. Pierrel F, Hernandez HL, Johnson MK, Fontecave M, Atta M. MiaB protein from Thermotoga maritima. Characterization of an extremely thermophilic tRNA-methylthiotransferase. J Biol Chem. 2003;278:29515–24.
48. Teske A, Callaghan AV, LaRowe DE. Biosphere frontiers of subsurface life in the sedimented hydrothermal system of Guaymas Basin. Front Microbiol 2014;5:362.
49. Schaefer M, Kapoor U, Jantsch MF. Understanding RNA modifications: the promises and technological bottlenecks of the 'epitranscriptome'. Open Biol. 2017;7:170077.
50. Laxman S, Sutter BM, Wu X, Kumar S, Guo X, Trudgian DC, et al. Sulfur amino acids regulate translational capacity and metabolic homeostasis through modulation of tRNA thiolation. Cell. 2013;154:416–42.
51. Thompson KM, Gottesman S. The MiaA tRNA modification enzyme is necessary for robust RpoS expression in *Escherichia coli*. J Bacteriol. 2014;196:754–61.

52. Teske A, Lizarralde D, Höfig TW, and the Expedition 385 Scientists. Guaymas Basin Tectonics and Biosphere. Proceedings of the International Ocean Discovery Program, 385: College Station, TX (International Ocean Discovery Program) (2021). https://doi.org/10.14379/iodp.proc.385.2021.
53. Cheng-Guang H, Gualerzi CO. The ribosome as a switchboard for bacterial stress response. Front Microbiol. 2021;11:619038.
54. Starnawski P, Bataillon T, Ettema TJ, Jochum LM, Schreiber L, Chen X, et al. Microbial community assembly and evolution in subseafloor sediment. Proc Natl Acad Sci USA. 2017;114:2940–5.
55. Kirkpatrick JB, Walsh EA, D'Hondt S. Microbial selection and survival in subseafloor sediment. Front Micro. 2019;10:9566.
56. Hui MP, Foley PL, Belasco JG. Messenger RNA degradation in bacterial cells. Annu Rev Genet. 2014;48:537–59.
57. Finkel SE, Kolter R. DNA as a nutrient: novel role for bacterial competence gene homologs. J Bacteriol. 2001;183:6288–93.
58. Jørgensen BB. Shrinking majority of the deep biosphere. Proc Natl Acad Sci USA. 2012;109:15976–7.
59. Biddle JF, Lipp JS, Lever MA, Lloyd KG, Sørensen KB, Anderson R et al. Heterotrophic archaea dominate sedimentary subsurface ecosystems off Peru. Proc Natl Acad Sci USA. 2006;103:3846–51.
60. Lynch M, Marinov GK. The bioenergetic costs of a gene. Proc Natl Acad Sci USA. 2015;11:15690–5.
61. Goyal M, Banerjee C, Nag S, Bandyopadhyay U. The Alba protein family: structure and function. Biochim Biophys Acta. 2016;1864:570–83.
62. Anantharaman V, Koonin EV, Aravind L. Comparative genomics and evolution of proteins involved in RNA metabolism. Nucleic Acids Res. 2002;30:1427–64.
63. Aravind L, Iyer LM, Anantharaman V. The two faces of Alba: the evolutionary connection between proteins participating in chromatin structure and RNA metabolism. Genome Biol. 2003;4:R64.
64. Gupta R, Laxman S. tRNA wobble-uridine modifications as amino acid sensors and regulators of cellular metabolic state. Curr Genet. 2020;66:475–80.
65. Droogmans L, Roovers M, Bujnicki JM, Tricot C, Hartsch T, Stalon V, et al. Cloning and characterization of tRNA (m1A58) methyltransferase (TrmI) from Thermus thermophilus HB27, a protein required for cell growth at extreme temperatures. Nucleic Acids Res. 2003;31:2148–56.
66. Kimura S, Suzuki T. Iron-sulfur proteins responsible for RNA modifications. Biochim Biophys Acta. 2015;1853:1272–83.
67. Gupta R, Walvekar AS, Liang S, Rashida Z, Shah P, Laxman S. A tRNA modification balances carbon and nitrogen metabolism by regulating phosphate homeostasis. eLife. 2019;8:e44795.
68. Heinemann IU, Söll D, Randau L. Transfer RNA processing in archaea: unusual pathways and enzymes. FEBS Lett. 2010;584:303–9.
69. Middelboe M, Glud RN, Wenzhöfer F, Oguri K, Kitazato H. Spatial distribution and activity of viruses in the deep-sea sediments of Sagami Bay, Japan. Deep-Sea Res I. 2006;53:1–13.
70. Manini E, Luna GM, Corinaldesi C, Zeppilli D, Bortoluzzi G, Caramanna G, et al. Prokaryote diversity and virus abundance in shallow hydrothermal vents of the Mediterranean Sea (Panarea Island) and the Pacific Ocean (North Sulawesi-Indonesia). Microb Ecol 2008;55:626–39.
71. Zhou YL, Mara P, Vik D, Edgcomb VP, Sullivan MB, Wang Y. Ecogenomics reveals viral communities across the Challenger Deep oceanic trench. Commun Biol. 2022;5:1055.
72. Imlay JA. How obligatory is anaerobiosis? Mol Microbiol. 2008;68:801–4.
73. Arosio P, Elia L, Poli M. Ferritin, cellular iron storage and regulation. IUBMB Life. 2017;69:414–22.
74. Eelderink-Chen Z, Bosman J, Sartor F, Dodd AN, Kovács AT, Merrow M. A circadian clock in a nonphotosynthetic prokaryote. Sci Adv. 2021;7:eabe2086.
75. Hagelueken G, Wiehlmann L, Adams TM, Kolmar H, Heinz DW, Tümmler B, et al. Crystal structure of the electron transfer complex rubredoxin rubredoxin reductase of Pseudomonas aeruginosa. Proc Natl Acad Sci USA. 2007;104:12276–81.
76. Giessen TW, Orlando BJ, Verdegaal AA, Chambers MG, Gardener J, Bell DC, et al. Large protein organelles form a new iron sequestration system with high storage capacity. eLife. 2019;8:e46070.
77. Scholz F, Schmidt M, Hensen C, Eroglu S, Geilert S, Gutjahr M, et al. Shelf-to-basin iron shuttle in the Guaymas Basin, Gulf of California. Geochim Cosmochim Acta. 2019;261:76–92. 2019
78. Fauvet B, Rebeaud ME, Tiwari S, De Los Rios P, Goloubinoff P. Repair or degrade: the thermodynamic dilemma of cellular protein quality-control. Front Mol Biosci. 2021;8:768888.
79. Sharma SK, De los Rios P, Christen P, Lustig A, Goloubinoff P. The kinetic parameters and energy cost of the Hsp70 chaperone as a polypeptide unfoldase. Nat Chem Biol 2010;6:914–20.
80. Suzuki MT, Taylor LT, DeLong EF. Quantitative analysis of small-subunit rRNA genes in mixed microbial populations via 5′-nuclease assays. Appl Environ Microbiol. 2000;66:4605–14.
81. Chen S, Zhou Y, Chen Y, Gu J. fastp: an ultra-fast all-in-one FASTQ preprocessor. Bioinformatics. 2018;34:i884–90.
82. Grabherr MG, Haas BJ, Yassour M, Levin JZ, Thompson DA, Amit I, et al. Full-length transcriptome assembly from RNA-Seq data without a reference genome. Nat Biotechnol. 2011;29:644–52.
83. Buchfink B, Reuter K, Drost HG. Sensitive protein alignments at tree-of-life scale using DIAMOND. Nat Methods. 2021;18:366–8.
84. Salter SJ, Cox MJ, Turek EM, Calus ST, Cookson WO, Moffatt MF, et al. Reagent and laboratory contamination can critically impact sequence-based microbiome analyses. BMC Biol. 2014;12:87.
85. Hyatt D, Chen GL, Locascio PF, Land ML, Larimer FW, Hauser LJ. Prodigal: prokaryotic gene recognition and translation initiation site identification. Bmc Bioinforma. 2010;11:119.
86. Fu L, Niu B, Zhu Z, Wu S, Li W. CD-HIT: accelerated for clustering the next-generation sequencing data. Bioinformatics. 2012;28:3150–2.
87. Aramaki T, Blanc-Mathieu R, Endo H, Ohkubo K, Kanehisa M, Goto S, et al. KofamKOALA: KEGG ortholog assignment based on profile HMM and adaptive score threshold. Bioinformatics. 2019;36:2251–2.
88. Kanehisa M, Sato Y, Morishima K. BlastKOALA and GhostKOALA: KEGG tools for functional characterization of genome and metagenome sequences. J Mol Biol 2016;428:726–31.
89. Patro R, Duggal G, Love MI, Irizarry RA, Kingsford C. Salmon provides fast and bias-aware quantification of transcript expression. Nat Methods. 2017;14:417–9.
90. Urbach E, Vergin KL, Young L, Morse A, Larson GL, Giovannoni SJ. Unusual bacterioplankton community structure in ultra-oligotrophic Crater Lake. Limnol Oceanogr 2001;46:557–72.
91. Takai K, Horikoshi K. Rapid detection and quantification of members of the archaeal community by quantitative PCR using fluorogenic probes. Appl Environ Microbiol. 2000;66:5066–72.
92. Boylen E, Rideout JR, Dillon MR, Bokulich NA, Abnet CC, Al-Ghalith GA, et al. Reproducible, interactive, scalable and extensible microbiome data science using QIIME 2. Nat Biotechnol. 2019;37:852–7.
93. Bokulich NA, Kaehler BD, Rideout JR, Dillon M, Bolyen E, Knight R, et al. Optimizing taxonomic classification of marker-gene amplicon sequences with QIIME 2's q2-feature-classifier plugin. Microbiome. 2018;6:90.
94. Quast C, Pruesse E, Yilmaz P, Gerken J, Schweer T, Yarza P, et al. The SILVA ribosomal RNA gene database project: improved data processing and web-based tools. Nucleic Acids Res. 2013;41:D590–6.
95. Morono Y, Terada T, Kallmeyer J, Inagaki F. An improved cell separation technique for marine subsurface sediments: applications for high-throughput analysis using flow cytometry and cell sorting. Environ Microbiol 2013;15:2841–9.
96. Kallmeyer J, Smith DC, Spivack AJ, D'Hondt S. New cell extraction procedure applied to deep subsurface sediments. LO Methods. 2008;6:236–45.
97. Inagaki F, Hinrichs KU, Kubo Y, Bowles MW, Heuer VB, Hong WL, et al. Exploring deep microbial life in coal-bearing sediment down to ~2.5 km below the ocean floor. Science. 2015;349:420–4.
98. Morono Y, Terada T, Masui N, Inagaki F. Discriminative detection and enumeration of microbial life in marine subsurface sediments. ISME J. 2009;3:503–11.
99. Zhou YL, Mara P. Analysis of the deep biosphere metatranscriptomes. *Zenodo* Accessed 2023. https://doi.org/10.5281/zenodo.7710615

ACKNOWLEDGEMENTS

We would like to acknowledge the crew and entire science party for IODP Expedition 385 for their assistance with sample collection. Without their assistance this study would have been impossible. We thank Dr. Daniel Lizarralde (WHOI) for the edited bathymetric map of Guaymas Basin. We also thank Takeshi Terada and Megumi Becchaku for assisting with cell counting. This study was supported by the National Science Foundation Grant OCE-2046799 to VE, PM, AT, R. Hatzenpichler, and OCE-1829903 to VE, PM, and AT, JSPS KAKENHI JP19H00730 and JP23H00154 to YM, and China Postdoctoral Science Foundation (2022M720039) and Guangdong Natural Resources Foundation (GDNRC[2023]30) to Y-LZ.

AUTHOR CONTRIBUTIONS

VE, AT and PM conceived of the experiments and designed the sampling strategy for analyses discussed in this paper. AT served as Co-Chief Scientist for IODP Expedition 385. VE collected samples for this study, with assistance from other IODP 385 shipboard microbiologists. YM performed cell counts, and provided cell count data and cell count figures. PM extracted RNA from samples for metatranscriptome analyses and DNA for the 16S rRNA marker gene analyses. PM, Y-LZ and DB analyzed metatranscriptome data. PM and Y-LZ analyzed marker gene data. PM, VE, AT, YM discussed data interpretation. PM wrote the first draft of the paper and all authors contributed to its final form.

COMPETING INTERESTS

The authors declare no competing interests.

ADDITIONAL INFORMATION

Supplementary information The online version contains supplementary material available at https://doi.org/10.1038/s41396-023-01492-z.

Correspondence and requests for materials should be addressed to Virginia Edgcomb.